2018 5th International Workshop on Compressed Sensing applied to Radar, Multimodal Sensing, and Imaging (CoSeRa)

Low-Rank Plus Sparse Decomposition, Multi-Chromatic Analysis and Generalized Likelihood Ratio Test for Ship Weak Detection, (L+S)-MCA-GLRT

Dr. Filippo Biondi, *Member, IEEE*

***Abstract*—The problem of obtaining stable motion estimation of maritime targets is that sea clutter makes wake structure detection and reconnaissance difficult. This article reports a focused study on the detection of ship wakes using the low-rank plus sparse decomposition (LRSD) combined with the generalized likelihood ratio test (GLRT) approach. The proposed algorithm is assisted by multichromatic analysis (MCA) used to whiten non-Gaussian sea clutter. Chirp subbands are generated for approximating Gaussianity of the sea clutter. Results are estimated on one set of COSMO-SkyMed satellite system stripmap data revealing excellent detection performance with respect to the state-of-the-art method.**

***Index Terms*—Synthetic Aperture Radar, Low-rank plus sparse decomposition, Multi chromatic analysis.**

I. Introduction

THIS article explains a novel detection method based on low-rank plus sparse decomposition (LRSD) algorithm implemented by Convex Programming (CP) combined with the generalized likelihood ratio test (GLRT) algorithm to detect sea wakes useful to retrieve the motion parameters, like root and velocity of maritime targets sailing over the open sea. LRSD, GLRT, and multichromatic analysis (MCA) are combined together, forming the low-rank plus sparse MCA GLRT ((L+S)-MCA-GLRT) algorithm where details and performance are explained in the methodology and experiments sections, respectively. Results are processed using only one patch of synthetic aperture radar (SAR) image representing a maritime target generating some wakes. In general, the wakes from surface ships seem to fall principally into four categories [1], these are: The Kelvin wake, the turbulent wake, wakes from internal waves, and narrow-V wakes. The problem for obtaining stable maritime targets motion estimation is that sea clutter makes difficult wakes structure detection and reconnaissance. Sea clutter is short-time stationary but long-time nonstationary, this means that it is locally homogeneous but globally inhomogeneous [2]. When these two assumptions do not hold, adaptive detectors suffer from a sharp degradation in performance [3]. Finding weak moving targets, such as small boats in sea clutter, requires a long integration time. The conflict between having long integration time and short homogeneous range span of sea clutter is the main obstacle for detecting weak moving targets. To overcome this problem chirp and Doppler subapertures are used to convert non-Gaussian sea clutter [4] in a pseudo-Gaussian version. This SAR processing is performed applying the multichromatic analysis (MCA) approach where the radar raw data are focused in multiple subapertures. The total chirp and Doppler bands are split into multiple overlapped subapertures, the narrower band raw subproducts are focused in lower resolution with respect to the original. Before exploiting details of the (L+S)-MCA-GLRT detector a short revisit of the LRSD, the GLRT and the MCA will be provided. In this article, the identification of the abovementioned features is made by performing a precious chirp subaperture analysis, assisted by LRSD which has been implemented by compressed sensing (CS). The application of CS in the radar field is consolidated in [5], where the technique demonstrates great potential in overcoming major limitations, in terms of spatial resolution, processing time, and onboard memory saving. When the CS technique in radar is used, the sparsity condition is the principal constraint that has to be overcome. Radar data are sparse when immersed in appropriate bases. This encourages the seeking of sparse-inducing transformations based on time-frequency analysis. Other successful applications of CS applied to the radar field are also theorized in [6-7]. In [8], following [9], LRSD has been applied for the first time in the field of maritime surveillance where the separation performance was excellent, under heavy clutter and also for small or larger maritime targets. Ship wakes often appear in synthetic aperture radar (SAR). In [10], a sensitivity analysis of a GLRT-based processor designed to detect coherent pulse trains in Weibull-distributed clutter-dominated environment was developed. Results demonstrate the suitability of the proposed strategy as a means for circumventing the a priori environmental uncertainty. Pioneering works performed on MCA [11-12] were made to resolve the 2π ambiguity of the interferometric SAR wrapped phase to avoid the ill-posed phase unwrapping computational stage. In [13], a computer simulation model for SAR of ship wakes for various configuration has been designed to study wake patterns observed with different SAR performance. The work showed that high-resolution SAR performs better than lower resolution in terms of detection performance. The work performed in [14] first described the distinctive features of ship wakes observed by SAR images. Experiments were performed using SEASAT and SIR-B radar images. In [15], a computer simulation of SAR L-band images of surface ship wakes has been provided. The model used in the simulation accounts for both the disturbance produced in the water by the moving

(c) EUSASIP 2018 / CoSeRa 2018

2018 5th International Workshop on Compressed Sensing applied to Radar, Multimodal Sensing, and Imaging (CoSeRa)

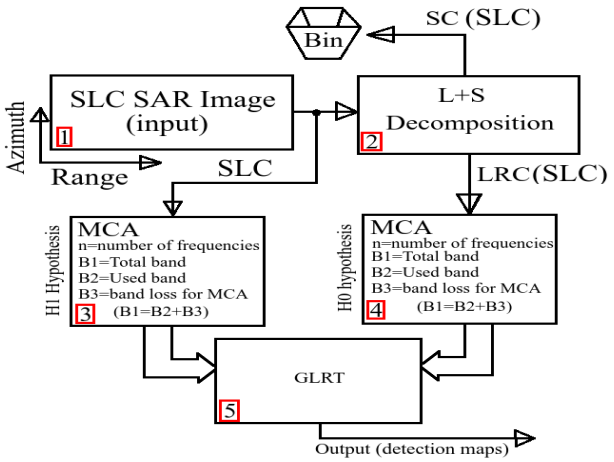

Fig. 1. (L+S)-MCA-GLRT computational scheme.

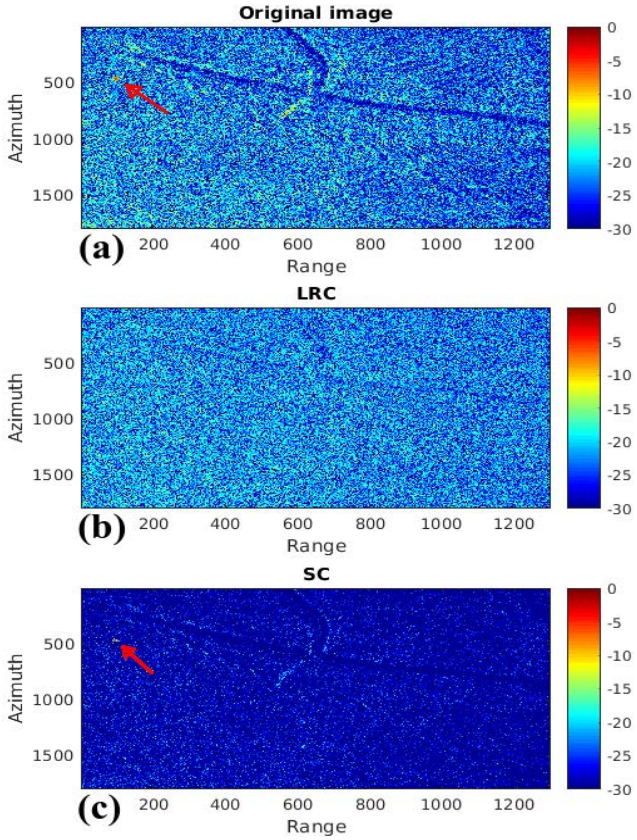

Fig. 2. ROI. (a): original image. (b): LRC. (c): SC.

ship and the influence of the background sea. In [16], a work focused to estimate the ship beam and its velocity by processing SAR images of the Kelvin and turbulent wakes has been proposed. The work implements the fast discrete RT to estimate the wakes pattern. In [17], a group of Kelvin wakes is simulated using the Michell theory. The random sea surface is simulated using the Pierson-Moskowitz type wave spectrum. The maritime target motion parameters are estimated using a discrete RT on order to detect the boundaries of the simulated Kelvin wakes. In [18], an RT-based approach to the detection of ship wakes in SAR images is reported. The RT is performed over short line segments, and a linear feature detection algorithm assisted by RT is developed. Results demonstrate the robustness of wake detection in presence of noise. In [19], the authors theorized detection of oil spills from multipolarization synthetic aperture radar images. In this article, the combination of CS with matrix completion for LRSD has been implemented to separate wakes generated by maritime targets by the rest of the SAR image background. Such decomposition was performed using robust principal component analysis to recover the principal components of a data matrix that were corrupted by missing entries. Results show excellent separation of the ship wakes with respect to the background, permitting the successful application of the Radon transform and the automatic estimation of the motion parameters.

II. Methodology

a) LRSD Model Presentation: A SAR sensor, after having compressed the RAW radar data in the range-azimuth directions and after having processed the motion compensation computational stage, produces a picture consisting of a matrix $M \in \mathbb{C}$. A great interest is decomposing the image in the following LRC and SC [9]:

$$\mathbf{M} = \mathbf{L} + \mathbf{S}. \tag{1}$$

In (1) $\mathbf{L}$ is a LR matrix and $\mathbf{S}$ is a sparse matrix and both have arbitrary in-phase (I) and quadrature-phase (Q) magnitudes. The LRC low-dimensional columns and its row-space are unknown. The SC number, locations and the I Q magnitudes of its non-zero elements are unknown. Considering a SAR image, it is of great interest to identify activities that stand out from the background. The result generates the $\mathbf{L}$, low-dimensional component which easily corresponds to the stationary background. The SC $\mathbf{S}$ is a perturbation generated by the moving objects that move like sprites over the background. Given a complex SAR image, having n_1 and n_2 range azimuth dimensions, $\mathbf{M}_{(I,Q)} \in \mathbb{R}^{n_1 \times n_2}$ for both I, Q components, the following convex optimization problem is considered [9]:

$$\underset{A,B}{\text{minimize}} = ||\mathbf{L}||_* + \gamma||\mathbf{S}||_{\ell_1}, \text{ s.t. } \mathbf{M} = \mathbf{L} + \mathbf{S}. \tag{2}$$

Algorithm (2) is also called principal component pursuit (PCP). In (2), the parameter γ balances the contribution of the ℓ_1-norm term which is relative to the nuclear norm term. The parameter $||\mathbf{L}||_* = \sum_j \sigma_j(\mathbf{L})$ is the nuclear norm of the matrix $\mathbf{L}$ defined as the sum of its singular values. The parameter $||\mathbf{S}||_{\ell_1} = \sum_{ij} \sigma_{ij} \mid \mathbf{S}_{ij}|$ is the ℓ_1-norm of $\mathbf{S}$, defined as the vector in $\mathbb{R}^{n_1 \times n_2}$ To implement an efficient algorithm that effectuates the LRSD of the unique $\mathbf{M}$ matrix, it is necessary to suppose that the $\mathbf{L}$ matrix is non-sparse and incoherent with the standard base. In each row and column the sparse matrix $\mathbf{S}$ should not contain a great number of non-zero elements.

b) Solution of the LRSD problem: The solution to the main problem can be summarized in the first instance by the

(c) EUSASIP 2018 / CoSeRa 2018

following singular value decomposition (SVD) formula [9]:

$$\mathbf{L} = (\mathbf{U}\mathbf{\Sigma}\mathbf{V}^*) = \sum_{i=1}^{r} \sigma_i u_i v_i^*. \tag{3}$$

In (3), the parameter r is the rank of the matrix $\mathbf{L}$, the parameters $[\sigma_1, \sigma_2, ..., \sigma_n]$ are the singular values and the matrices $\mathbf{U} = [u_1, u_2, ..., u_r]$ and $\mathbf{V} = [v_1, v_2, ..., v_r]$ are the left and right singular vectors. It is evident that problem (3) is ill-posed. In extremely unfavorable conditions, a convex optimization solution is highly recommended to be used. The application of LRSD will produce the $\mathbf{L}$ matrix which represents the back-scattered image and the $\mathbf{S}$ matrix. The $\mathbf{S}$ matrix represents the pixel variation that occurs from column to column. It is necessary to define the standing following an incoherent condition, having parameter μ [9]:

$$\max_i ||\mathbf{U}^* \cdot e_i||^2 \leq \frac{\mu_r}{n_1}, \quad \max_i ||\mathbf{V}^* \cdot e_i||^2 \leq \frac{\mu_r}{n_2}, \tag{4}$$
$$||\mathbf{U}\mathbf{V} \cdot e_i||_\infty \leq \sqrt{\frac{\mu_r}{n_1 \cdot n_2}}.$$

In (4) the ℓ_∞-norm parameter $||\mathbf{M}||_\infty = \max_{ij}|\mathbf{M}|_{ij}$ term is a long vector and the parameters $\mathbf{U}^*$ and $\mathbf{V}^*$ are the orthogonal projections $\mathbf{P}_U$ and $\mathbf{P}_V$ in the U and V column spaces respectively. For small values of the parameter μ, the singular vectors are not sparse. A non negligible problem emerges when the SC is also the LR and the algorithm presents difficulty in defining sparsity or incoherence. This condition will occur if all the non-zero entries of $\mathbf{S}$ are located in a few columns. To avoid these indetermination issues, the algorithm will assume that the sparsity pattern is uniformly and randomly selected. However, where the matrix $\mathbf{L}_0$ has $n \times n$ dimensionality, obeying (4), and its SCs $\mathbf{S}_0$ has a support set uniformly distributed along all cardinal sets, a constant parameter c exists, such that, with probability $P = 1 - cn^{-10}$, the PCP separation algorithm will exactly recover $\mathbf{L} = \mathbf{L}_0$ and $\mathbf{S} = \mathbf{S}_0$ with $\lambda = \frac{1}{\sqrt{n}}$. It is also assumed that

$$\text{rank}(L_0) \leq \rho_r n \mu^{-1} (\log n)^{-2} \text{ and } m \leq \rho_s n^2. \tag{5}$$

In (5), the parameters ρ_r and ρ_s, are positive numerical constants. For general rectangular case, where the dimensionality of $\mathbf{L} = \mathbf{L}_0$ is $n_1 \times n_2$, the algorithm provides exact recovery for $\lambda = \frac{1}{\sqrt{n_{max}}}$ [9]. A schematic representation of the dual-stage algorithm is represented in Fig.1.

c) Multi-chromatic-analysis problem formulation: MCA split the overall range spectral bandwidth B_1 of the SAR image into multiple sub-bands $B_1 ... B_N$ centered at different N carrier frequencies. The MCA technique can be used to measure absolute interferometric angles starting from wrapped interferometric maps estimated cross-multiplying the corrisponding masters and slaves sub-look images [11-12]. In the case of this paper the MCA approach has been used to transform non-Gaussian sea clutter in its pseudo-Gaussian version.

d) (L+S)-MCA-GLRT: The energy of the maritime target and the wakes can be modeled considering the covariance matrix (CM) estimated in H independent looks $M_1 \in \mathbb{C}^{\mathbb{H} \times \mathbb{H}}$. In the case of observing only sea clutter the energy collected by the CM will be lower. The detection problem can be formulated in terms of following hypothesis test [3]:

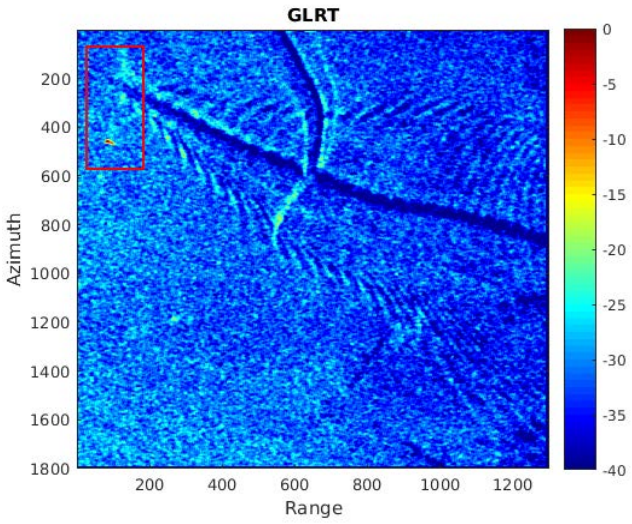

Fig. 3. Positive GLRT detection map.

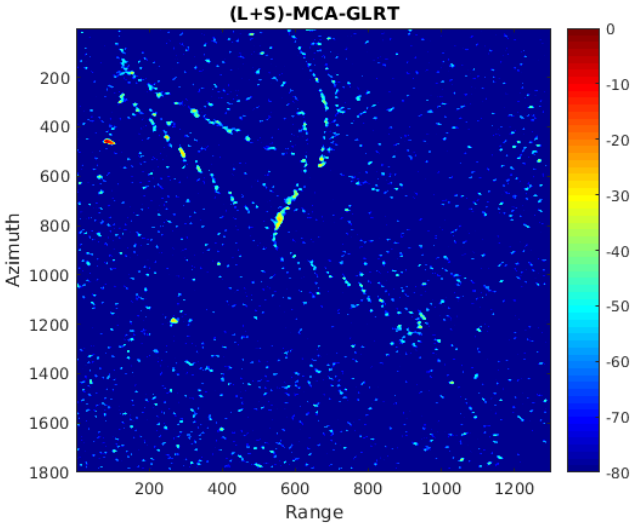

Fig. 4. Positive (L+S)-MCA-GLRT detection map.

$$\mathcal{H}_0 = w_n = \text{LRC} \tag{6}$$
$$\mathcal{H}_1 = \text{SC} + w_n = \text{LRC} + \text{SC} = \text{SLC}.$$

This model requires only one ROI because the input data of the hypothesis $\mathcal{H}_0$ is estimated by the LRC. The GLRT test is repeated for all the chirp sub-aperture images produced for all the frequencies.

III. Experimental Results

In this work, one stripmap image observed by the COSMO-SkyMed satellite system has been processed. The SAR image has a resolution of 3 m in the range and azimuth directions. Fig. 2 (a) shows the selected ROI, in which one maritime target (indicated by a red arrow) can be detected, along with the wakes it produced. The ship is focused delocalized from the wakes vertex because during the SAR Doppler integration time

(c) EUSASIP 2018 / CoSeRa 2018

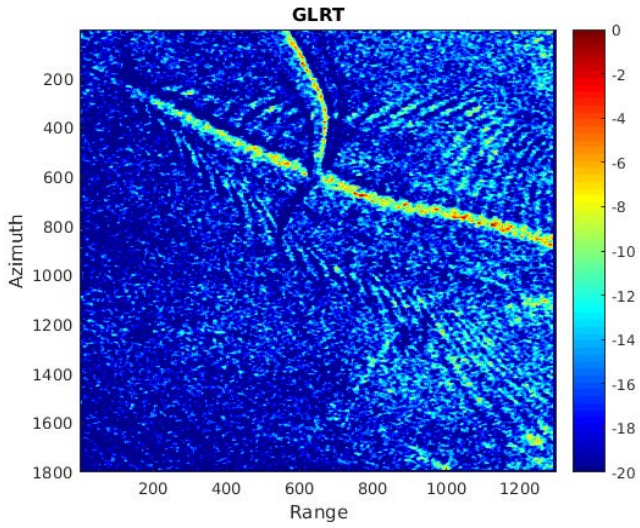

Fig. 5. Negative GLRT detection map.

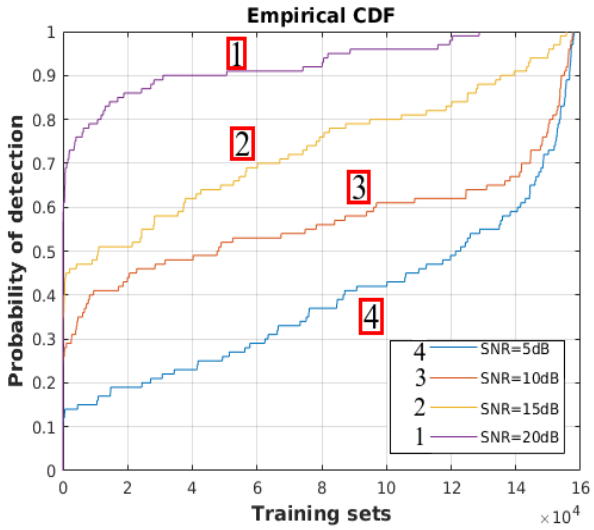

Fig. 8. CDFs at different SNR levels.

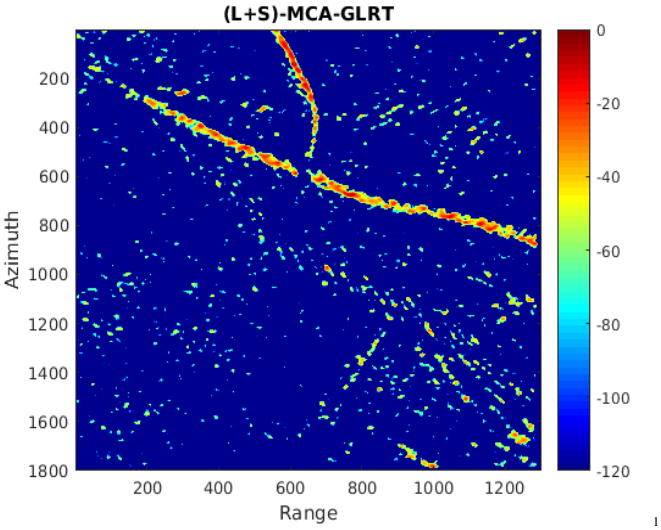

Fig. 6. Negative (L+S)-MCA-GLRT detection map.

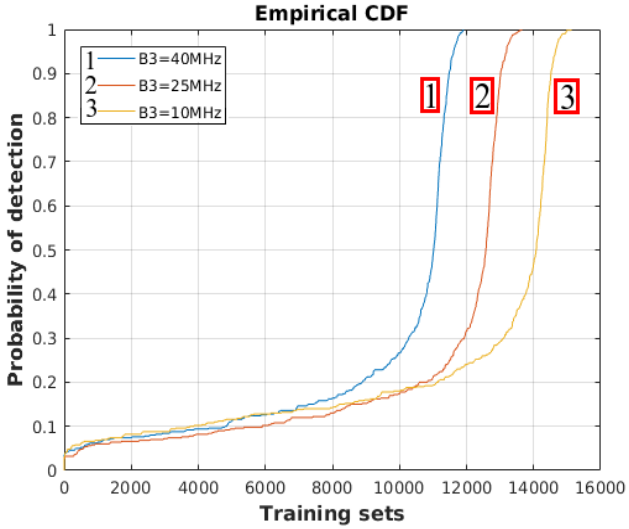

Fig. 9. CDFs at different bands.

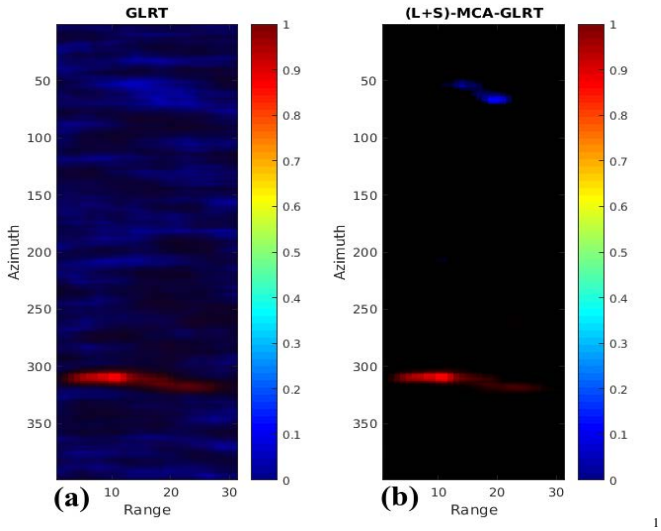

Fig. 7. GLRT results. (a): Positive GLRT (red) and negative GLRT (blue). (b): Positive (L+S)-MCA-GLRT (red) and negative (L+S)-MCA-GLRT (blue).

was observed on non-null relative velocity range component with respect to the sensor motion. By measuring this gap distance, it is possible to estimate the velocity component in the range direction. To estimate the velocity component in the azimuth direction, the frequency of the transverse waves needs to be determined. Removing the sea background from such sparse objects in the image and GLRT can be a suitable solution to enhance the reconnaissance of a maritime target and the wakes it produced. The model is found to work in the present case, and it has not been observed that the algorithm is robust also when the weather condition changes. The experimental results provide support that the presented algorithm enhances the tracking capabilities for maritime targets. Fig. 1 shows the computational scheme used to produce all the results shown in this article. Each computational block (CB) is labeled by a number. The SLC ROI is produced by CB number 1. This result is given to CB number 2, which is designed to compute the LRSD. The input of this stage consists of

(c) EUSASIP 2018 / CoSeRa 2018

one SLC ROI of the SAR image. The L+S decomposition computational stage applies the LRSD algorithm to separate the SC from the LRC. The SC ROI map is not used, and only the LRC inputs the next digital RT computational stage. The results are based on one study case in which the ROI consists of a marine target and the generated wake pattern. This complex environment is extrapolated from the background sea by applying the LRSD. The results of CB number 2 indicate that the above-explained LRSD algorithm achieved excellent background subtraction. Fig. 2 (a) represents the original SAR image. Fig. 2 (b and c) are the LRC and the SC of the original image, respectively. The MCA analysis is computed by the computational stages number 3 and number 4. The MCA computational stages were set according to the following parameters: The stripmap image is focused using 80 MHz of chirp band. The author set the generation of 200 MCA subproducts focused at lower resolution and setting $B_1 = 40MHz$, $B_2 = 25MHz$, $B_3 = 10MHz$. The multiple outputs of the MCA computational stages are imputed in the GLRT CM number 5. The (L+S)-MCA-GLRT results are compared with the one estimated by the standard GLRT algorithm. Fig. 3 shows the positive GLRT result and Fig. 4 is the positive (L+S)-MCA-GLRT detection map. Results of standard GLRT offers high quantity of false alarms at -40 dB of energy threshold, the (L+S)-MCA-GLRT detection map has very little false alarms at -80 dB, and the wakes structure is detected. Fig. 5 and Fig. 6 are the negative GLRT and (L+S)-MCA-GLRT results, respectively. Results of standard negative GLRT confirm a high quantity of false alarms at -20 dB and the (L+S)-MCA-GLRT negative detection map confirms very little false alarms at -120 dB and the central structure of the wakes is also detected. Fig. 7 is the particular of the maritime target (red box of Fig. 3). (L+S)-MCA-GLRT algorithm is able to detect the target together to the shadow (Fig. 7 (b)) with respect to a noise result estimated by the standard GLRT depicted in Fig.7 (a). Fig. 8 and Fig. 9 represent the validation of the (L+S)-MCA-GLRT performance algorithm. The results are estimated using simulated data where one synthetic target has been embedded in Rayleigh noise. Fig. 8 is the cumulative distribution function (CDF) representing the probability of detection versus signal to noise ratio (SNR). The study found an improvement of the detection probability increasing the SNR (Fig.8) and the band chirp sacrificed to generate the MCA (Fig.9).

IV. Conclusions

This article explains a novel detection method based on LRSD algorithm implemented by CP combined with the GLRT algorithm to detect sea wakes useful to retrieve the motion parameters, such as root and velocity of maritime targets sailing over the open sea. LRSD, GLRT, and MCA were combined together forming the (L+S)-MCA-GLRT algorithm where results were estimated using only one patch of SAR image representing a maritime target generating some wakes. In this article, the combination of CS with matrix completion for LRSD has been implemented to separate wakes generated by maritime targets by the rest of the SAR image background. Such decomposition was performed using robust principal component analysis to recover the principal components of a data matrix that were corrupted by missing entries. Results show excellent separation of the ship wakes with respect to the background, permitting the successful application of the Radon transform and the automatic estimation of the motion parameters. The study found an improvement of the detection probability increasing the SNR and the band chirp sacrificed to generate the MCA.

References

[1] J. K. E. Tunaley; E. H. Buller; K. H. Wu; M. T. Rey, The simulation of the SAR image of a ship wake, *IEEE Trans. on Geosc. and Remote Sensing*, Year: 1991, Volume: 29, Issue: 1, Pages: 149 - 156.

[2] A. M. Reed, R. F. Beck, O. M. Griffin, and R. D. Peltzer, Hydrodynamics of remotely sensed surface ship wakes, *IEEE Trans. Soc. Nav. Arch. Marine Eng*, vol. 99, pp. 319363, 1990.

[3] E. Conte; A. De Maio; and G. Ricci, Recursive estimation of the covariance matrix of the compound-Gaussian process and its applications to adaptive CFAR detection, *IEEE Trans. on Signal Proc.*, 50, 8 (2002), 19081915.

[4] G. Picardi, Elaborazione del segnale radar. Metodologie ed applicazioni, Franco Angeli, year 1995, EAN: 9788820489304.

[5] R. Baraniuk, P. Steeghs Compressive Radar Imaging, *IEEE radar conference 2007* pages 128-133, Boston MA. DOI: 11.1109/RADAR.2007.374203. Print ISBN: 1-4244-0284-0. INSPEC A.N.: 973094. ISSN:1097-5659. Pages: 128-133. April 2007.

[6] R. Baraniuk, P. Steeghs Compressive Radar Imaging, *IEEE radar conference 2007* pages 128-133, Boston MA.

[7] F. Biondi, Compressed Sensing Radar, New Concepts of Continuous Wave Transmissions, *2016 4th Int. Workshop on Compressed Sensing Theory and its Applications to Radar, Sonar and Remote Sensing (CoSeRa)*, 204 208, 17-19 June 2015.

[8] F. Biondi, Low rank plus sparse decomposition of synthetic aperture radar data for maritime surveillance, *2016 4th Int. Workshop on Compressed Sensing Theory and its Applications to Radar, Sonar and Remote Sensing (CoSeRa)*, Year: 2016, Pages: 75 - 79.

[9] E. J. Candes and Y. Plan. Tight oracle bounds for low-rank matrix recovery from a minimal number of random measurements. *IEEE Transactions on Information Theory,* 57(4), 2342-2359.

[10] E. Conte; G. Ricci, Sensitivity study of GLRT detection in compound-Gaussian clutter, *IEEE Transactions on Aerospace and Electronic Systems*, Year: 1998, Volume: 34, Issue: 1, Pages: 308 - 316.

[11] S. N. Madsen; H. A. Zebker. Automated Absolute Phase Retrieval in Across-Track Interferometry. *Geosc. and Remote Sensing Symposium, 1992. IGARSS '92. Int.*, Year: 1992, Volume: 2. Pages: 1582 - 1584.

[12] F. Bovenga; V. M. Giacovazzo; A. Refice; N. Veneziani. Multichromatic Analysis of InSAR Data, *IEEE Transactions on Geoscience and Remote Sensing*. Year: 2013, Volume: 51, Issue: 9. Pages: 4790 - 4799.

[13] K. Oumansour; Y. Wang; J. Saillard, Multifrequency SAR observation of a ship wake, IEEE *Proceedings - Radar, Sonar and Navigation*, Year: 1996, Volume: 143, Issue: 4, Pages: 275 - 280.

[14] A. Reed; D. Taylor; R.F. Beck; O. M. Griffin; R.D. Peltzer, Hydrodynamics of Remotely Sensed Surface Ship Wakes, *SNAME Transactions*, Vol. 98, 1990, pp. 319-363.

[15] J. K. E. Tunaley; E. H. Buller; K. H. Wu; M. T. Rey, The simulation of the SAR image of a ship wake, *IEEE Transactions on Geosc. and Remote Sensing*, Year: 1991, Volume: 29, Issue: 1, Pages: 149 - 156.

[16] G. Zilman; A. Zapolski; M. Marom, The speed and beam of a ship from its wakes SAR images *IEEE Trans. on Geoscience and Remote Sensing*, Year: 2004, Volume: 42, Issue: 10 Pages: 2335 - 2343.

[17] G. Zilman; A. Zapolski; M. Marom, On Detectability of a Ships Kelvin Wake in Simulated SAR Images of Rough Sea Surface, *IEEE Transactions on Geoscience and Remote Sensing*, Year: 2015, Volume: 53, Issue: 2, Pages: 609 - 619.

[18] M. T. Rey, J. K. E. Tunaley, J. T. Folinsbee, P. A. Jahans, J. A. Dixon, and M. R. Vant, Application of Radon transform techniques to wake detection in Seasat-A SAR images, *IEEE Trans. Geosci. Remote Sensing*, vol. 28, pp. 553-560, July 1990.

[19] A. De Maio; D. Orlando; L. Pallotta; C. Clemente, A Multifamily GLRT for Oil Spill Detection, *IEEE Trans. on Geos. and Rem. Sens.*, Year: 2017, Volume: 55, Issue: 1, Pages: 63 - 79.

(c) EUSASIP 2018 / CoSeRa 2018